Yuzuncu Yil University
Journal of Agricultural Sciences
(Yüzüncü Yıl Üniversitesi Tarım Bilimleri Dergisi)
https://dergipark.org.tr/en/pub/yyutbd

ISSN: 1308-7576 e-ISSN: 1308-7584

Research Article

In Silico Determination of The Antifungal Effect of Plant Active Molecules Against *Botrytis Cinerea* by Molecular Docking

Vildan Enisoglu ATALAY*[1], Beyza YILMAZ[2], Mehmet Emin URAS[3]

[1]Informatics Institute, Computational Science and Engineering, Istanbul Technical University, TR-34469 Istanbul, Türkiye
[2]Uskudar University, Faculty of Engineering and Natural Sciences, Department of Molecular Biology and Genetics, 34662, Istanbul, Türkiye
[3]Haliç University, Faculty of Sciences and Arts, Department of Molecular Biology and Genetics, 34060, Istanbul, Türkiye

[1]https://orcid.org/0000-0002-5086-7265, [2]https://orcid.org/0009-0007-5768-5070, [3]https://orcid.org/0000-0002-0444-9994

*Corresponding author e-mail: enisogluatalayv@itu.edu.tr

Article Info

Received: 20.10.2023
Accepted: 23.04.2024
Online published: 15.06.2024
DOI: 10.29133/yyutbd.1377395

Keywords

Biopesticides,
Botrytis cinerea,
Molecular Docking,
QSAR parameters

Abstract: *Botrytis cinerea*, which has developed many strategies to infect plants, can survive in harsh environmental conditions, and has a wide host range, has become an important problem both economically and ecologically by causing tons of crop losses for many years. The residues in soil and crops caused by chemical pesticides used to get rid of agricultural pests pose serious threats to human and environmental health, such as hormonal abnormalities and acute respiratory poisoning, especially in children. The most critical step to avoid these hazards will be to replace chemical pesticides with plant-active molecules. At the same time, these studies primarily in silico will provide a return in terms of both time and cost. Inhibition of pectin methyl esterase, an important virulence factor of *B. cinerea*, will ensure the organism is controlled. In order to determine candidate biofungicide effector molecules, QSAR parameter values of 409 plant active molecules were calculated. Firstly, conformer distribution and geometry optimizations were performed with Spartan 14' software. Docking studies of the optimized molecules were carried out through Autodock Vina software, while visualization studies to make sense of the interactions between the target receptor structure and effector molecules were used by BIOVIA Discovery Studio software. As a result of all the analyses, the molecules that are alternatives to chemical pesticides as biofungicides were determined to be the following molecules: Podolactone B, Repin, Sandaracopimaradienediol, 6-Hydrogenistein, Artemisinin, Lycoricidine, 6-Methoxygossypol, Viscidulin, Ciprofloxacin, and 7,4'-Dihydroxyflavan.

To Cite: Atalay, V E, Yilmaz, B, Uras, M E, 2024. *In Silico* Determination of The Antifungal Effect of Plant Active Molecules Against *Botrytis Cinerea* by Molecular Docking. *Yuzuncu Yil University Journal of Agricultural Sciences*, 34(2): 323-334.
DOI: https://doi.org/10.29133/yyutbd.1377395

1. Introduction

Fungi, also referred to as plant pathogens due to the infections they cause on various plant species, have developed numerous strategies to infect plants and these relationships result in a series of processes ranging from beneficial interactions to the death of the host organisms (Williamson et al.,

2007). Pathogenic fungi cause a variety of diseases in plants, such as powdery mildew, root rot or blight, and gray mold in many vegetable and fruit species (tomatoes, cucumbers, onions, grapes, strawberries, pears, bananas, kiwifruit, etc.), which reduce crop productivity or have the potential to completely destroy the related crops (Mathew et al., 2021).

Botrytis cinerea and other *Botrytis* species are important plant pathogens with a wide range of host plants in temperate regions, especially nursery crops, vegetables, ornamentals, and field and orchard crops also store and transport agricultural products. *B. cinerea*, which is among the top 10 pathogens worldwide and ranks 2nd in terms of economic damage, has been reported to cause different diseases such as gray mold, root blight, and root and storage rot in more than 200 plant species, including most vegetable and fruit crops, trees and flowers (Dean et al., 2012). They can attack many parts of the host organism including leaves, stems, and fruit parts of infected plants as necrotrophs, and often cause heavy losses after harvest (Youssef et al., 2019). They can also be found as saprophytes on immunocompromised or dead plant material. Table 1 arranges information about the common organisms of B. cinerea.

Table 1. Hosts of *B. cinerea* pest

Scientific Name	Common Name	References
Vitis vinifera	Grape	(Latorre et al., 2015)
Solanum lycopersicum	Tomato	(Boukaew et al., 2017)
Pyrus communis	Pear	(Kurbetli et al., 2016)
Fragaria vesca	Strawberry	(Petrasch et al., 2019)
Actinidia deliciosa	Kiwifruit	(Karakaya and Bayraktar, 2009)
Rubus idaeus	Raspberry	(Dean et al., 2012)
Allium cepa	Onion	(Chilvers, 2006)
Solanum tuberosum	Potato	(Sun et al., 2017)
Cucumis sativus	Cucumber	(Sadek et al., 2022)
Ipomoea batatas	Sweet Potato	(Stahr and Quesada-Ocampo, 2019)
Cucurbita moschata	Yellow Squash	(Hawthorne, 1988)
Capsicum annuum	Bell Paper	(Wang et al., 2022)
Daucus carota	Carrot	(Stahr and Quesada-Ocampo, 2019)

B. cinerea is a highly successful pathogen due to its flexible infection strategies, high reproductive efficiency, wide host range, and ability to survive for long periods as small mycelial structures called conidia and/or sclerotia. (Abbey et al., 2019) reported that *B. cinerea* initiates invasion of host plants through damaged tissues or natural openings, enabling the fungus to establish infection. Although the initial infected tissue usually results in minor damage, there is a rapid spread of the fungus as a result of intensive conidia production (Viret et al., 2004). Researchers have described the primary infection step of *B. cinerea* as the formation and air transportation of asexual conidia spores from mature conidiophores. After the initial infection, *B. cinerea* enters a short phase in which it exists as a biotroph within the plant (Williamson et al., 2007), *B. cinerea* has been reported to enter an aggressive necrotrophic phase in maturing host tissues, which is suggested to be triggered by biochemical changes such as an increase in volatile organic compounds, sugar, and nitrogen content (Prusky and Lichter, 2007).

The effects of virulence factors on hosts are characterized by fruit rot resulting in the softening of the fruit section and brown, leathery skin (Xiao, 2006). A further pathophysiological consequence of infection is that *B. cinerea* itself undergoes rapid mycelial growth on plant surfaces and forms massive masses of gray conidia, causing necrosis of tissues and even loss of host organism viability.

Cell wall-degrading enzymes play a critical role in *B. cinerea* as they allow penetration through plant cell walls and degradation of host tissue after infection. Pectin methylesterase 1 (PME1) is secreted early in the penetration phase to hydrolyze pectin, an important plant cell wall component. Pectin methylesterases therefore catalyze the demethylesterification of homogalacturonan, rendering pectin degradable by polygalacturonases and pectate lyases (Nakajima and Akutsu, 2014). In mutant studies, the pme1 deletion mutant was reported to exhibit a fourfold decrease in PME activity. As a result, PME activity was found to be reduced by 75% in the Bcpme1 mutant (Valette-Collet et al., 2003).

Unfortunately, resistant varieties to *Botrytis* species are not available, chemical control remains the primary means of reducing the incidence of gray mold in major crops. However, due to the development of multidrug resistance in field strains of the fungus, this strategy is only partially successful. Researchers have made great efforts to understand the mechanisms of pathogenicity of this pathogen due to its wide host range and the severe damage it causes in agriculture. Anti-Botrytis products, used as a preventive measure against *Botrytis*, which can infect crops before or after harvest, have reached a market size of €1 billion in recent years. At the same time, Botrytis species have been reported to cause 10-70% crop losses before and after harvest (Elad et al., 2019).

Despite the availability of technologies for the early detection of gray mold infection developed in recent years (Sunil et al., 2023; Chun et al., 2024), the physical and financial damage to agricultural crops caused by the *B. cinerea* pathogen remains significant today (Rojas and Gilbert, 2024) due to limitations in their application in the field (Bock et al., 2020).

Using biofungicides containing plant active molecules instead of chemical fungicides to prevent plant damage caused by fungi, which are plant pathogens, plays an important role in agriculture and food protection due to their non-toxic nature, rapid biodegradability, absence of chemical residues, and focus on managing the host structure rather than destroying it. Through their distinct metabolic pathways, plants can synthesize chemicals, and these compounds have shown the potential to be employed in the treatment and prevention of diseases that are caused by microorganisms (Demirel et al., 2022). The development of new biological fungicide molecules prevent the damages caused by chemical-containing pesticides used to avoid these damages and to protect crop productivity for both the host organism and the soil structure will lead to the elimination of ecological threats to the environment and human health. Spending $1 on the use of pesticides for plant protection purposes generates a profit of $3-5 (Pimentel et al., 1978; Pimentel et al., 1991). In studies investigating the pesticidal activity of plant-derived molecules to replace chemical pesticide molecules, molecular docking method, which allows detailed analysis of the infection mechanisms of pathogens, is frequently used and these results overlap with their experimental data (Ez-Zoubi et al., 2023; Diab et al., 2024; Vivekanandhan et al., 2024).

In this study, calculations were made through in silico methods, similar to our previous fungi study (Atalay and Asar, 2024). In order to understand the structure-activity relationship and to analyze the action mechanism of the fungistic molecules, the physicochemical parameters of the active ones with candidate antifungals were determined, and according to the obtained results, established a relationship between molecular structures and protein targets. Considering the fact that the protein structure used in the study was selected for plant pests and the scope of the analyses performed, it is predicted that determining the active molecules primarily in silico will provide great progress in terms of time and cost in both experimental and commercialization studies.

2. Material and Methods

Through the Dr. Duke database (Duke, 2020), 600 plant active molecules with antifungal properties were identified. In order to make a comparison with these selected plant active molecules, 9 commercial fungicides (CFs) (Azoxystrobin, Boscalid, Cyprodinil, Fenhexamid, Fluazinam, Imazalil, Penthiopyrad, Pyraclostrobin, Pyrimethanil) molecules against *B. cinerea* pest were included in the study (TOB, 2023). The SwissADME database (Daina et al., 2017) was used to predict the drug-likeness and ADME (absorption, distribution, metabolism, and excretion) properties of plant active molecules to evaluate their potential as candidate biofungicide effector molecules. After 600 molecules were identified in the first studies, it was adjusted to 409 molecules based on their compatibility with Lipinski parameters (Lipinski et al., 1997). Conformer distribution and geometry optimizations of all molecules with the Molecular Mechanics/MMFF and Semi-Empirical PM6 methods, respectively, using Spartan'14 software (Hehre, 2003). Molecular weight (M_W) (amu); area (A^2); volume (A^3); partition coefficient (logP); dipole moment (μ) (debye) and polarizability (α) values were calculated and recorded for structure-activity relationship modeling.

In this study, in order to establish more comprehensive relationships between physicochemical parameters and biological activity to make detailed analyses, in addition to the parameters calculated in

Spartan software, electronegativity (χ), electrophilicity (ω) chemical properties were calculated using equations (1) and (2).

$$\chi = (E_{HOMO}+E_{LUMO})/2 \quad (1)$$

$$\omega = \chi^2 / 2*\eta \quad (2)$$

Researchers obtained the three-dimensional crystallographic structure of the protein with Uniprot accession number Q9C2Y1, which consists of 346 amino acids, through the AlphaFold database (Jumper et al., 2021). In molecular docking studies, the binding site coordinates of the protein were chosen as x = 17.673, y = 5.457, z = -3.031, and the grid box size 40x40x40 $Å^3$ with 0.375 Å grid space. Molecular docking studies were performed with Autodock Tools 1.5.6 (Morris et al., 2009) and Autodock Vina (Eberhardt et al., 2021) software. Table 2 abbreviates the binding energy values obtained from docking studies as BE. After the molecular docking studies, visualization was performed using the BIOVIA Discovery Studio program (Biovia, 2021).

3. Results

In order to perform more comprehensive analyses to establish meaningful relationships between the molecule set and protein structure, linear regression analyses were performed by keeping the BE values constant. The calculated physicochemical parameter values of 164 correlated plant active molecules and CFs also their the inhibition constants represented by K_i of these molecules in the target protein structure are given in Table 2 and the R^2 values obtained as a result of regression studies are given in Table 3.

Table 2. Computed physicochemical parameters and BE values

Effector Molecules	A^2	A^3	M_W	χ	ω	α	μ	logP	BE	K_i
CF-1 (Azoxystrobin)	426.7	402.1	403.4	9.9	439.1	72.0	3.71	0.91	-6.1	$3.4x10^{-5}$
CF-2 (Boscalid)	336.9	321.1	343.2	9.7	397.6	65.6	2.79	1.12	-6.7	$1.2x10^{-5}$
CF-3 (Cyprodinil)	273.1	250.9	225.3	8.6	310.4	59.8	1.63	2.19	-6.3	$2.4x10^{-5}$
CF-4 (Fenhexamid)	296.4	280.5	302.2	9.0	338.7	62.2	3.25	1.09	-5.6	$7.8x10^{-5}$
CF-5 (Fluazinam)	346.4	321.6	465.1	11.5	590.8	65.7	1.24	-2.75	-6.6	$1.5x10^{-5}$
CF-6 (Imazalil)	312.6	285.8	297.2	9.7	420.5	62.6	4.37	1.38	-5.2	$1.5x10^{-4}$
CF-7 (Penthiopyrad)	367.2	339.5	359.4	8.9	322.3	67.1	9.29	3.15	-6.4	$2x10^{-5}$
CF-8 (Pyraclostrobin)	399.6	375.1	387.8	9.1	340.2	70.0	2.25	1.29	-7.6	$2.7x10^{-6}$
CF-9 (Pyrimethanil)	242.6	220.9	199.3	8.6	308.8	57.4	1.78	1.47	-6.5	$1.7x10^{-5}$
L-323 (Podolactone B)	350.2	354.1	394.4	11.4	652.8	67.9	2.07	-1.76	-11.8	$2.24x10^{-9}$
L-56 (Aminolevulinic Acid)	162.2	130.7	131.1	9.6	452.3	49.7	3.04	-1.21	-10.7	$1.43x10^{-8}$
L-340 (Repin)	360.1	351.8	362.4	10.7	582.5	67.6	6.67	-0.37	-10.6	$1.7x10^{-8}$
L-353 (Sandaracopimaradienediol)	333.1	342.5	304.5	8.7	380.7	67.7	3.49	4.09	-10.2	$3.33x10^{-8}$
L-12 (3,8'-Biapigenin)	486.4	489.0	538.5	9.8	400.7	79.2	7.89	-5.73	-9.9	$5.53x10^{-8}$
L-277 (Narciclasine)	283.5	268.4	307.4	9.8	411.3	61.2	6.06	-4.94	-9.9	$5.53x10^{-8}$
L-28 (6-Hydroxygenistein)	272.2	260.5	286.2	9.5	377.1	60.7	1.23	-3.11	-9.9	$5.53x10^{-8}$
L-71 (Artemisinin)	281.0	277.0	282.3	9.8	457.8	61.7	6.99	2.86	-9.8	$6.54x10^{-8}$
L-145 (Cumambrin B)	277.1	270.1	264.3	9.7	435.5	61.1	4.87	0.63	-9.7	$7.75x10^{-8}$
L-162 (Desacetoxymatricarin)	267.4	257.6	246.3	10.1	492.9	60.0	5.58	2.28	-9.7	$7.75x10^{-8}$
L-259 (Lycoricidine)	275.1	261.2	291.3	9.7	405.9	60.7	5.81	-3.88	-9.7	$7.75x10^{-8}$
L-40 (Achillin)	266.1	257.1	246.3	10.0	490.9	60.0	5.34	2.28	-9.7	$7.75x10^{-8}$
L-29 (6-Methoxygossypol)	517.2	527.3	532.6	9.2	323.6	82.5	9.81	-4.02	-9.5	$1.09x10^{-7}$
L-57 (Ampelopsin)	297.1	280.4	320.3	9.6	391.7	62.2	1.35	-4.97	-9.5	$1.09x10^{-7}$
L-400 (Viscidulin C)	279.1	269.2	264.3	9.7	483.2	60.7	6.90	0.48	-9.4	$1.29x10^{-7}$
L-128 (Ciprofloxacin)	333.2	320.6	331.3	9.0	336.9	65.5	9.34	-1.63	-9.3	$1.52x10^{-7}$
L-31 (7,4'-Dihydroxyflavan)	264.9	249.6	242.3	8.7	326.0	59.6	1.88	-0.60	-9.2	$1.8x10^{-7}$
L-369 (Solstitialin)	289.0	278.2	280.3	10.1	522.6	61.5	3.78	-0.11	-9.2	$1.8x10^{-7}$
L-227 (Ilicic Acid)	284.9	274.8	252.4	10.3	530.2	61.3	1.96	2.75	-8.9	$2.99x10^{-7}$
L-80 (Avenalumin III)	319.5	299.7	291.3	9.6	376.0	63.9	1.43	1.21	-8.9	$2.99x10^{-7}$

Table 2. Computed physicochemical parameters and BE values (continued)

Effector Molecules	A^2	A^3	M_W	χ	ω	α	μ	logP	BE	K_i
L-151 (Daidzin)	407.9	386.9	416.4	9.3	362.2	70.9	3.23	-2.94	-8.8	$3.54x10^{-7}$
L-182 (Epigallocatechin Gallate)	427.9	407.4	458.4	9.4	374.8	72.6	1.63	-6.72	-8.8	$3.54x10^{-7}$
L-23 (6,6'-Dimethoxygossypol)	536.2	546.7	546.6	9.1	313.2	84.1	8.42	-3.92	-8.8	$3.54x10^{-7}$
L-63 (Anhydrotuberosin)	329.1	319.6	320.3	8.4	274.5	65.6	3.39	-2.62	-8.8	$3.54x10^{-7}$
L-203 (Glyceocarpin)	354.6	341.0	340.4	9.0	365.1	66.9	4.29	-1.89	-8.7	$4.19x10^{-7}$
L-81 (Azetidine-2-Carboxylic-Acid)	125.8	101.8	101.1	9.6	456.0	47.3	2.06	-0.68	-8.7	$4.19x10^{-7}$
L-136 (Coniferin)	334.8	321.2	342.3	9.0	331.4	65.6	11.86	-1.63	-8.6	$4.96x10^{-7}$
L-255 (Liquiritin)	416.6	392.1	418.4	9.8	436.3	71.1	5.53	-3.06	-8.6	$4.96x10^{-7}$
L-89 (Bayogenin)	598.3	649.4	650.9	9.0	387.4	91.7	3.64	3.72	-8.6	$4.96x10^{-7}$
L-201 (Genistein)	265.3	253.4	270.2	8.5	342.2	60.0	1.66	-2.03	-8.5	$5.87x10^{-7}$
L-204 (Glyceofuran)	353.6	340.3	354.4	9.1	359.9	67.0	2.50	-3.96	-8.5	$5.87x10^{-7}$
L-13 (3-Hydroxyuridine)	252.2	225.1	260.2	10.5	525.5	57.5	3.10	-2.19	-8.4	$6.95x10^{-7}$
L-160 (Demethylvestitol)	269.1	256.2	258.3	8.6	314.3	60.2	3.90	-1.81	-8.4	$6.95x10^{-7}$
L-215 (Hildecarpin)	312.8	300.9	330.3	8.9	330.5	63.9	2.39	-4.98	-8.4	$6.95x10^{-7}$
L-267 (Medicarpin)	279.2	267.6	270.3	8.8	335.1	61.0	0.78	-2.27	-8.4	$6.95x10^{-7}$
L-278 (Naringenin)	272.5	258.2	272.3	9.8	434.6	60.3	2.51	-2.15	-8.4	$6.95x10^{-7}$
L-314 (Pinnatin)	397.4	289.8	292.3	9.4	367.1	63.0	2.74	-1.28	-8.4	$6.95x10^{-7}$
L-389 (Trifolirhizin)	424.2	405.8	446.4	8.8	324.5	72.4	2.00	-5.21	-8.4	$6.95x10^{-7}$
L-82 (Baicalein)	266.0	253.7	270.2	9.6	386.9	60.1	3.89	-2.38	-8.4	$6.95x10^{-7}$
L-24 (6,7-Dihydroxyflavone)	261.6	247.7	254.2	9.7	404.6	59.6	2.55	-1.29	-8.3	$8.23x10^{-7}$
L-67 (Apiocarpin)	340.7	331.8	338.4	9.1	369.3	66.2	2.48	-2.84	-8.3	$8.23x10^{-7}$
L-7 (2,3-Dehydrokievitone)	357.7	345.9	354.4	9.4	365.8	67.6	3.37	-1.83	-8.3	$8.23x10^{-7}$
L-121 (Catechin)	288.4	271.5	290.3	9.2	375.5	61.4	3.77	-3.72	-8.2	$9.74x10^{-7}$
L-205 (Glyceollin-I)	341.0	331.5	338.4	9.0	354.5	66.3	2.93	-2.63	-8.2	$9.74x10^{-7}$
L-234 (Isoliquiritin)	423.4	396.8	418.4	9.9	426.0	71.6	3.35	-2.33	-8.2	$9.74x10^{-7}$
L-266 (Medicagol)	273.7	263.9	296.2	9.4	357.8	61.0	2.93	-3.97	-8.2	$9.74x10^{-7}$
L-61 (Anhydroglycinol)	254.9	243.2	254.2	8.7	297.1	59.3	0.63	-3.17	-8.2	$9.74x10^{-7}$
L-117 (Carnosol)	336.6	339.6	330.4	9.2	371.4	66.9	6.51	1.77	-8.1	$1.15x10^{-6}$
L-156 (Dehydromaackiain)	371.0	261.5	282.3	8.7	300.8	60.8	1.53	-4.01	-8.1	$1.15x10^{-6}$
L-158 (Demethylmedicarpin)	259.2	247.5	256.3	9.0	362.5	59.4	1.36	-2.38	-8.1	$1.15x10^{-6}$
L-285 (Nordihydroguaiaretic Acid)	331.3	320.0	302.4	8.5	300.2	65.4	5.36	0.11	-8.1	$1.15x10^{-6}$
L-34 (9-O-Methylcoumestrol)	278.7	265.7	282.3	9.3	347.5	61.2	4.52	-3.03	-8.1	$1.15x10^{-6}$
L-398 (Vestitol)	290.0	276.3	272.3	8.5	305.3	61.8	5.04	-1.70	-8.1	$1.15x10^{-6}$
L-45 (Agaroxin-A)	508.8	508.9	519.6	8.9	341.9	80.7	5.04	-4.09	-8.1	$1.15x10^{-6}$
L-79 (Avenalumin II)	305.4	287.3	279.3	9.7	400.3	62.8	2.72	0.80	-8.1	$1.15x10^{-6}$
L-147 (Curcumin)	409.2	378.3	368.4	9.3	356.5	70.2	1.05	-0.46	-8.0	$1.37x10^{-6}$
L-148 (Cyclokievitone)	350.6	341.1	354.4	8.9	342.5	67.1	4.50	-2.64	-8.0	$1.37x10^{-6}$
L-164 (Dianthalexin)	249.1	234.5	239.2	10.3	470.2	58.4	3.48	0.18	-8.0	$1.37x10^{-6}$
L-192 (Flavanone)	249.4	237.6	224.3	9.6	415.3	58.6	2.75	1.10	-8.0	$1.37x10^{-6}$
L-311 (Piceatannol)	267.3	245.0	244.2	9.1	343.8	59.4	2.01	-1.71	-8.0	$1.37x10^{-6}$
L-312 (Piceid)	397.1	376.4	390.4	9.0	342.4	60.0	1.00	-2.62	-8.0	$1.37x10^{-6}$
L-315 (Pinocembrin)	263.3	250.9	256.3	9.8	439.9	59.6	2.51	-1.06	-8.0	$1.37x10^{-6}$
L-36 (Acanthocarpan)	298.2	291.5	328.3	9.0	340.1	63.1	1.36	-4.84	-8.0	$1.37x10^{-6}$
L-379 (Tetrahydroxystilbene)	265.6	244.4	244.2	9.2	371.2	59.2	0.96	-1.71	-8.0	$1.37x10^{-6}$
L-77 (Astringin)	402.1	383.0	406.4	9.0	334.8	70.6	2.44	-3.70	-8.0	$1.37x10^{-6}$
L-306 (Phebalosin)	278.6	263.9	258.3	9.9	429.8	60.9	3.88	-0.41	-7.9	$1.62x10^{-6}$
L-338 (Quercetin)	281.2	267.9	302.2	9.5	365.6	61.3	0.89	-4.54	-7.9	$1.62x10^{-6}$
L-106 (Cajanol)	318.8	304.9	316.3	9.2	377.4	64.1	1.51	-2.97	-7.8	$1.91x10^{-6}$
L-25 (6-Alpha-Hydroxymaackiain)	283.1	273.4	300.3	9.2	356.2	61.6	2.54	-4.01	-7.8	$1.91x10^{-6}$
L-305 (Pheanthine)	618.7	644.4	622.8	8.1	264.6	91.8	6.03	-3.91	-7.8	$1.91x10^{-6}$
L-351 (Sakuranetin)	293.6	278.4	286.3	9.6	419.5	61.9	2.46	-2.04	-7.8	$1.91x10^{-6}$

Table 2. Computed physicochemical parameters and BE values (continued)

Effector Molecules	A_2	A^3	M_W	χ	ω	α	μ	logP	BE	K_i
L-385 (Tiliacorinine)	546.2	582.9	576.7	8.5	294.1	86.8	3.56	-4.02	-7.8	$1.91x10^{-6}$
L-46 (Aglafoline)	496.4	488.7	492.5	9.0	362.1	78.9	3.12	-2.70	-7.8	$1.91x10^{-6}$
L-62 (Anhydropisatin)	292.1	281.7	296.3	8.6	287.7	62.5	1.80	-3.90	-7.8	$1.91x10^{-6}$
L-105 (Cajanin)	290.7	279.6	300.3	9.4	366.5	62.2	3.79	-3.01	-7.7	$2.27x10^{-6}$
L-134 (Clandestacarpin)	340.2	328.6	336.3	9.1	356.1	66.1	1.98	-3.11	-7.7	$2.27x10^{-6}$
L-207 (Glyceollin-III)	343.5	332.7	338.4	8.9	348.7	66.3	3.55	-2.55	-7.7	$2.27x10^{-6}$
L-9 (2'-Hydroxydaidzein)	264.7	253.3	270.2	9.3	359.4	60.1	3.88	-2.03	-7.7	$2.27x10^{-6}$
L-110 (Canescacarpin)	340.8	330.3	336.3	9.4	386.4	66.2	5.11	-2.26	-7.6	$2.68x10^{-6}$
L-221 (Honokiol)	319.3	298.8	266.3	8.9	342.9	63.6	1.83	1.43	-7.6	$2.68x10^{-6}$
L-223 (Hordatine B)	622.4	593.1	580.7	9.0	340.9	87.6	5.57	-3.64	-7.6	$2.68x10^{-6}$
L-303 (Phaseolin)	333.4	324.0	322.4	8.8	333.0	65.7	1.46	-1.83	-7.6	$2.68x10^{-6}$
L-316 (Pinostrobin)	284.3	271.0	270.3	9.6	419.5	61.3	2.15	-0.96	-7.6	$2.68x10^{-6}$
L-342 (Resveratrol)	259.1	237.8	228.2	9.1	356.6	58.7	1.77	-0.62	-7.6	$2.68x10^{-6}$
L-382 (Theaflavin)	487.7	502.6	564.5	9.5	363.3	80.5	3.12	-7.56	-7.6	$2.68x10^{-6}$
L-386 (Trichocarpin)	402.2	385.1	406.4	10.0	446.6	70.7	2.68	-2.17	-7.6	$2.68x10^{-6}$
L-399 (Vestitone)	289.2	277.8	286.3	9.2	354.6	62.0	2.89	1.93	-7.6	$2.68x10^{-6}$
L-10 (2'-Hydroxygenistein)	269.7	259.4	286.2	9.5	378.3	60.6	2.52	-3.11	-7.5	$3.18x10^{-6}$
L-177 (Dolichin-B)	354.9	341.0	340.4	8.8	335.2	67.0	1.88	-2.14	-7.5	$3.18x10^{-6}$
L-254 (Liquiritigenin)	267.7	252.2	256.3	9.7	424.6	59.8	4.20	-1.06	-7.5	$3.18x10^{-6}$
L-318 (Pisatin)	304.2	293.6	314.3	9.1	346.9	63.3	1.83	-3.90	-7.5	$3.18x10^{-6}$
L-33 (8-Methoxypsoralen)	220.0	206.7	216.2	9.3	349.7	56.4	6.13	-1.65	-7.5	$3.18x10^{-6}$
L-65 (Anonaine)	269.4	268.4	265.3	8.9	327.0	61.2	1.09	-1.24	-7.5	$3.18x10^{-6}$
L-95 (Betagarin)	330.6	317.3	328.3	8.8	326.0	65.2	2.21	-2.77	-7.5	$3.18x10^{-6}$
L-170 (Dihydroresveratrol)	261.5	241.8	230.3	8.9	351.9	58.9	0.31	-0.30	-7.4	$3.76x10^{-6}$
L-228 (Integerrine)	600.4	619.9	593.7	8.5	302.9	89.7	4.47	-0.67	-7.4	$3.76x10^{-6}$
L-252 (Limacine)	608.0	626.0	608.7	7.9	244.3	90.3	8.36	-4.02	-7.4	$3.76x10^{-6}$
L-317 (Pinosylvin)	249.9	230.5	212.2	9.4	387.4	58.1	1.62	0.46	-7.4	$3.76x10^{-6}$
L-332 (Psoralidin)	344.8	331.7	336.3	9.3	350.4	66.5	5.61	-1.85	-7.4	$3.76x10^{-6}$
L-367 (Solasodine)	449.3	456.9	413.6	8.3	327.7	76.0	1.40	4.95	-7.4	$3.76x10^{-6}$
L-403 (Withaferin A)	462.0	480.2	470.6	10.2	499.6	78.1	7.91	3.46	-7.4	$3.76x10^{-6}$
L-44 (Afrormosin)	309.8	294.8	298.3	9.0	329.3	63.5	1.82	-1.82	-7.4	$3.76x10^{-6}$
L-6 (1-Tuliposide-B)	275.4	262.9	294.3	10.6	550.6	60.5	2.76	-2.71	-7.4	$3.76x10^{-6}$
L-208 (Glyceollin-IV)	376.5	361.2	354.4	8.7	329.4	68.6	2.31	-1.78	-7.3	$4.45x10^{-6}$
L-226 (Hydroxyphaseolin)	340.1	331.2	338.4	9.0	350.6	66.2	1.70	-2.63	-7.3	$4.45x10^{-6}$
L-104 (Caffeic Acid)	199.6	174.7	180.2	9.6	396.1	53.7	3.87	-0.86	-7.2	$5.27x10^{-6}$
L-176 (Dolichin-A)	355.0	341.1	340.4	8.8	336.3	67.0	0.70	-2.14	-7.2	$5.27x10^{-6}$
L-206 (Glyceollin-II)	340.0	331.1	338.4	8.9	332.7	66.3	2.96	-2.63	-7.2	$5.27x10^{-6}$
L-142 (Cristacarpin)	375.6	361.5	354.4	8.9	354.9	68.6	3.74	-1.78	-7.1	$6.24x10^{-6}$
L-292 (Oxypeucedanin)	297.4	281.3	286.3	9.7	404.6	62.3	7.44	-1.53	-7.1	$6.24x10^{-6}$
L-251 (Licoisoflavone A)	355.6	345.4	354.4	9.4	363.0	67.6	0.86	-1.83	-7.0	$7.39x10^{-6}$
L-66 (Antofine)	383.5	382.1	363.5	8.2	260.3	70.6	2.22	-1.69	-7.0	$7.39x10^{-6}$
L-86 (Batatasin-II)	305.0	288.4	274.3	8.3	288.8	62.8	2.91	-1.17	-7.0	$7.39x10^{-6}$
L-180 (Ellipticine)	266.5	264.2	246.3	8.5	279.0	61.1	3.43	-0.57	-6.9	$8.74x10^{-6}$
L-244 (Juglone)	178.3	166.9	174.2	10.8	505.0	53.1	0.66	0.57	-6.9	$8.74x10^{-6}$
L-281 (Nimbidin)	404.6	438.6	442.6	9.0	383.8	74.7	4.18	1.59	-6.9	$8.74x10^{-6}$
L-102 (Broussonin A)	293.2	279.1	258.3	8.6	323.2	62.0	0.86	0.22	-6.8	$1.04x10^{-5}$
L-84 (Batatasin V)	326.0	308.2	288.3	8.5	309.4	64.3	3.12	-1.07	-6.8	$1.04x10^{-5}$
L-249 (Lathodoratin)	215.8	199.0	206.2	9.9	450.1	55.5	1.92	-0.92	-6.7	$1.23x10^{-5}$
L-325 (Pogostone)	257.9	233.4	224.3	10.8	565.9	58.1	2.69	0.92	-6.7	$1.23x10^{-5}$
L-72 (Arvensan)	310.7	296.3	286.3	8.3	288.0	63.5	2.73	-1.59	-6.7	$1.23x10^{-5}$
L-194 (Frangufoline)	580.6	579.3	534.7	9.0	368.3	86.2	6.89	1.37	-6.6	$1.45x10^{-5}$

Table 2. Computed physicochemical parameters and BE values (continued)

Effector Molecules	A_2	A^3	Mw	χ	ω	α	μ	logP	BE	K_i
L-392 (Umbelliferone)	172.2	156.5	162.1	10.0	441.6	52.1	3.97	-0.58	-6.6	$1.45x10^{-5}$
L-124 (Chrysarobin)	246.1	239.4	240.3	9.8	422.4	58.8	5.21	-0.16	-6.5	$1.72x10^{-5}$
L-173 (Dihydrowyerone)	313.2	282.0	260.3	10.1	462.5	62.3	3.92	1.98	-6.5	$1.72x10^{-5}$
L-179 (Elemicin)	252.5	231.7	208.3	8.6	328.1	58.1	2.62	-0.64	-6.4	$2.03x10^{-5}$
L-276 (Myristicin)	224.3	203.2	192.2	8.6	322.1	55.8	1.23	-0.61	-6.4	$2.03x10^{-5}$
L-291 (Otobain)	334.9	330.2	324.4	8.5	312.9	66.1	1.39	-0.23	-6.4	$2.03x10^{-5}$
L-409 (Xyloidone)	256.0	244.4	240.3	10.0	420.3	59.4	0.92	1.12	-6.4	$2.03x10^{-5}$
L-52 (Allylpyrocatechol)	183.2	164.2	150.2	8.8	338.0	52.6	2.74	0.12	-6.4	$2.03x10^{-5}$
L-100 (Boa)	261.5	233.7	207.3	8.5	299.9	58.3	5.27	0.03	-6.3	$2.41x10^{-5}$
L-232 (Isoelemicin)	251.9	231.4	208.3	8.7	324.7	58.1	1.82	-0.69	-6.3	$2.41x10^{-5}$
L-83 (Batatasin III)	277.9	260.9	244.3	8.9	355.2	60.4	0.78	-0.20	-6.3	$2.41x10^{-5}$
L-195 (Frangulanine)	556.3	548.8	500.7	9.0	364.5	83.7	6.57	1.80	-6.2	$2.85x10^{-5}$
L-383 (Thujaplicin)	197.4	180.8	164.2	9.5	384.8	54.1	4.06	1.67	-6.1	$3.37x10^{-5}$
L-41 (Acoric Acid)	299.4	288.4	268.4	9.7	469.7	62.4	4.17	3.36	-6.1	$3.37x10^{-5}$
L-114 (Caprylic Acid)	206.0	172.4	144.2	10.9	688.2	52.6	2.13	2.43	-6.0	$4x10^{-5}$
L-289 (O-Methoxycinnamaldehyde)	200.6	180.1	162.2	9.3	391.9	53.9	4.88	0.07	-6.0	$4x10^{-5}$
L-212 (Helenalin)	270.0	264.9	262.3	10.6	558.8	60.6	4.92	2.00	-5.9	$4.73x10^{-5}$
L-384 (Thymol)	200.6	179.3	150.2	8.6	326.6	53.8	1.51	1.56	-5.9	$4.73x10^{-5}$
L-42 (Actinidine)	189.8	173.1	147.2	9.4	416.6	53.2	3.55	1.51	-5.9	$4.73x10^{-5}$
L-243 (Jodrellin A)	430.0	438.3	448.5	9.3	420.3	74.6	5.93	1.60	-5.8	$5.6x10^{-5}$
L-270 (Menthone)	206.7	187.4	154.3	9.3	438.8	54.1	3.49	3.07	-5.8	$5.6x10^{-5}$
L-70 (Arteannuin-B)	268.0	260.8	248.3	10.0	501.7	60.2	7.13	1.90	-5.8	$5.6x10^{-5}$
L-115 (Capsidiol)	276.4	268.0	236.4	9.4	446.3	60.6	1.79	2.37	-5.7	$6.63x10^{-5}$
L-224 (Humulone)	414.7	392.5	362.5	9.7	411.7	71.3	2.26	2.45	-5.7	$6.63x10^{-5}$
L-349 (Rugosal A)	272.1	273.3	266.3	9.7	415.6	61.5	4.43	1.41	-5.7	$6.63x10^{-5}$
L-377 (Terpinen-4-ol)	205.9	187.8	154.3	8.6	370.3	54.1	1.85	2.23	-5.7	$6.63x10^{-5}$
L-378 (Terpinolene)	194.2	175.7	136.2	7.9	296.6	53.2	0.49	2.81	-5.7	$6.63x10^{-5}$
L-131 (Citral)	219.2	191.8	152.2	9.4	414.6	54.7	5.21	2.35	-5.6	$7.85x10^{-5}$
L-132 (Citronellal)	223.6	196.1	154.3	9.1	396.1	54.9	3.25	2.36	-5.6	$7.85x10^{-5}$
L-401 (Warburganal)	266.4	267.6	250.3	10.0	467.2	60.9	4.49	1.71	-5.6	$7.85x10^{-5}$
L-126 (Cinnamaldehyde)	172.9	251.9	132.2	10.1	467.6	51.7	4.07	1.04	-5.5	$9.29x10^{-5}$
L-90 (Benzoic-Acid)	146.5	127.5	122.1	10.6	548.7	49.5	2.64	0.79	-5.5	$9.29x10^{-5}$
L-297 (Patchouli Alcohol)	247.8	254.2	222.4	8.3	383.7	59.0	1.76	3.85	-5.4	$1.1x10^{-4}$
L-394 (Undecylenic Acid)	261.7	223.6	184.3	9.8	502.5	57.0	1.75	3.42	-5.4	$1.1x10^{-4}$
L-93 (Benzyl-Isothiocyanate)	179.8	156.8	149.2	9.2	366.3	52.1	4.54	1.47	-5.4	$1.1x10^{-4}$
L-96 (Beta-Ionone)	252.0	232.6	192.3	9.3	400.7	58.0	3.82	3.43	-5.4	$1.1x10^{-4}$
L-113 (Capric Acid)	246.5	209.3	172.3	10.8	669.8	55.6	2.13	3.27	-5.3	$13x10^{-5}$
L-107 (Camphor)	188.8	176.4	152.2	9.1	418.5	53.2	3.44	2.92	-5.2	$1.54x10^{-4}$
L-37 (Acetophenone)	155.9	138.2	120.2	10.3	512.1	50.4	3.45	1.30	-5.2	$1.54x10^{-4}$
L-4 (1,8-Cineole)	195.3	182.1	154.3	8.0	345.8	53.3	1.60	1.86	-5.2	$1.54x10^{-4}$
L-133 (Citronellol)	230.4	201.1	156.3	8.3	339.4	55.2	1.66	2.82	-5.1	$1.83x10^{-4}$
L-368 (Solavetivone)	267.2	257.0	218.3	9.7	463.4	59.9	4.74	3.88	-5.1	$1.83x10^{-4}$

The R^2 values obtained as a result of linear regression analysis to identify candidate biofungicide active molecules are given in Table 3.

Table 3. Lineer regression results

Parameters	logP	ω	A^2	α	χ	Mw
R^2 values	0.8034	0.7677	0.7435	0.7359	0.7317	0.7188

4. Discussion

Several investigations using molecular docking programs have shown that using computational screening to rank the affinities of ligands binding to receptor proteins might lead to a greater enrichment of active molecules compared to random screening against plant pathogens such as viruses, fungi, and bacteria (Stahl and Rarey, 2001; Usta et al., 2023; Wyss et al., 2003).

Because of the large number of the studied molecules, the calculated parameter values followed a wide range of numbers within themselves. This allowed a detailed analysis of how and at what rate the binding energies change depending on the relevant parameters. For example; while the logP values of the CF used against *B. cinerea* were found to be in the range of $-2.75 \leq logP \leq 3.81$, the logP value ranges of the 409 plant active molecules studied were found to be $-7.56 \leq logP \leq 9.11$. In the linear regression analysis results, the highest correlation was observed in the logP parameter with the R^2 value of 0.8034 (Table 3). The logP value ranges of 172 candidate bioactive molecules that provide this correlation were determined as $-5.73 \leq logP \leq 4.95$. Plant active molecules with higher affinity than CFs had value ranges in the range of $-1.76 \leq logP \leq 2.86$ when evaluated together with BE values. As a result of these findings, it can be said that the determined target protein active site structure is lipophobic therefore hydrophilic. The recommended parameter value at the ranges in the studied PME inhibition mechanism was determined as $380 \leq \omega \leq 680$, $280 \leq M_W \leq 395$, $57 \leq \alpha \leq 68$, $250 \leq A^2 \leq 450$, $8.40 \leq \chi \leq 11.40$.

The interactions of the effector molecules with amino acids were analyzed by analyzing the active site of the selected receptor structure in the study for the inhibition of PME secreted by *B. cinerea* to break down the plant cell wall. For this, firstly, the interaction types and interaction distances of the effector molecules with the macromolecule in the interaction maps were collected as data (Supporting information). The conventional H bond interaction, which is considered the most critical interaction in intermolecular interactions, was taken as a reference in determining the critical amino acids in the active site. Figure 1 represents the interaction maps of proposed candidate molecules with active site amino acids. As a result of the information obtained, the amino acids expected to cause significant changes in protein structure and function in case of possible mutations in these amino acids in the receptor structure were determined as Gly301, Asn302, Thr303, Gly304, Ser307, Asn308, Ser309. The interaction distances of the critical amino acids in the active site with the effector molecules via conventional H bonds were observed to vary between 1.76-3.35 Å. Considering that the bond distance between intramolecular C-C atoms is 1.54 Å, it is possible to evaluate the observed conventional H bond interaction distances between the molecules as close interactions and this situation is closely related to the active site selectivity of the selected effector molecules. The contribution of this type of interaction to the BE values is quite high because the BE values increase as the interaction distances of the effector molecules with conventional H bond interactions shorten. In addition, when the chemical properties of the critical amino acids were analyzed, it was inferred that the receptor active site structure is mostly polar. This inference is consistent with the findings observed in the regression results of the logP parameter. Other essential results are the interaction maps, that the active site amino acids have remarkable interaction distances (2.70-3.37Å) with the candidate biofungicides, especially 6-Hydrogenistein, Artemisinin, and Lycoricidine. The named amino acids overlap above mentioned amino acids list as highlighted.

When the interaction tables are examined, after the conventional H bond interaction, π-alkyl, π-cation and π-π interactions were the most common interactions with apolar amino acids containing aliphatic R groups. Among these interactions, π-alkyl was observed with the amino acid Pro6 in the bond distance range of 3.45-5.21 Å, π-cation with the amino acid Leu4 in the bond distance range of 3.23-4.24 Å, and π-π interactions with the amino acid Ile5 in the bond distance range of 3.74-4.51 Å.

In order to verify the selectivity of the candidate biofungicide molecules in the active site of the target protein, they were compared with the amino acids interacting with the CFs included in the study as a reference. CFs interacted with Ile5, Pro6, Asn302, Ser307, and Ser309 amino acids in the active site. All the identified amino acids were also detected in candidate bio-fungicide molecules.

The BE values of CFs vary between -5.2 and -7.6 $kcal.mol^{-1}$, while the BE values of studied biofungicide active molecules vary between -5.1 and -11.8 $kcal.mol^{-1}$. Table 4 provides the coefficients of increase in binding affinity of alternative candidate bio fungicide active molecules against CF active molecules in the PME inhibition mechanism and the proposed molecules.

Table 4. Affinity differences between CFs and Candidate biofungicides

Candidate Biofungicide	Candidate Biofungicide BE (kcal.mol^{-1})	CFs	CFs BE (kcal.mol^{-1})	Affinity Difference	Number of Candidate Biofungicide≥CFs
L-323	-11.8	**CF-1**	-6.1	1.000-1.000.000	131
L-340	-10.6	**CF-2**	-6.7	300-126.000	118
L-353	-10.2	**CF-3**	-6.3	800-320.000	130
L-28	-9.9	**CF-4**	-5.6	4000-1.600.000	149
L-71	-9.8	**CF-5**	-6.6	400-160.000	121
L-259	-9.7	**CF-6**	-5.2	10.000-4.000.000	159
L-29	-9.5	**CF-7**	-6.4	600- 250.000	125
L-400	-9.4	**CF-8**	-7.6	40-16.000	78
L-128	-9.3	**CF-9**	-6.5	500-200.000	123
L-31	-9.2				

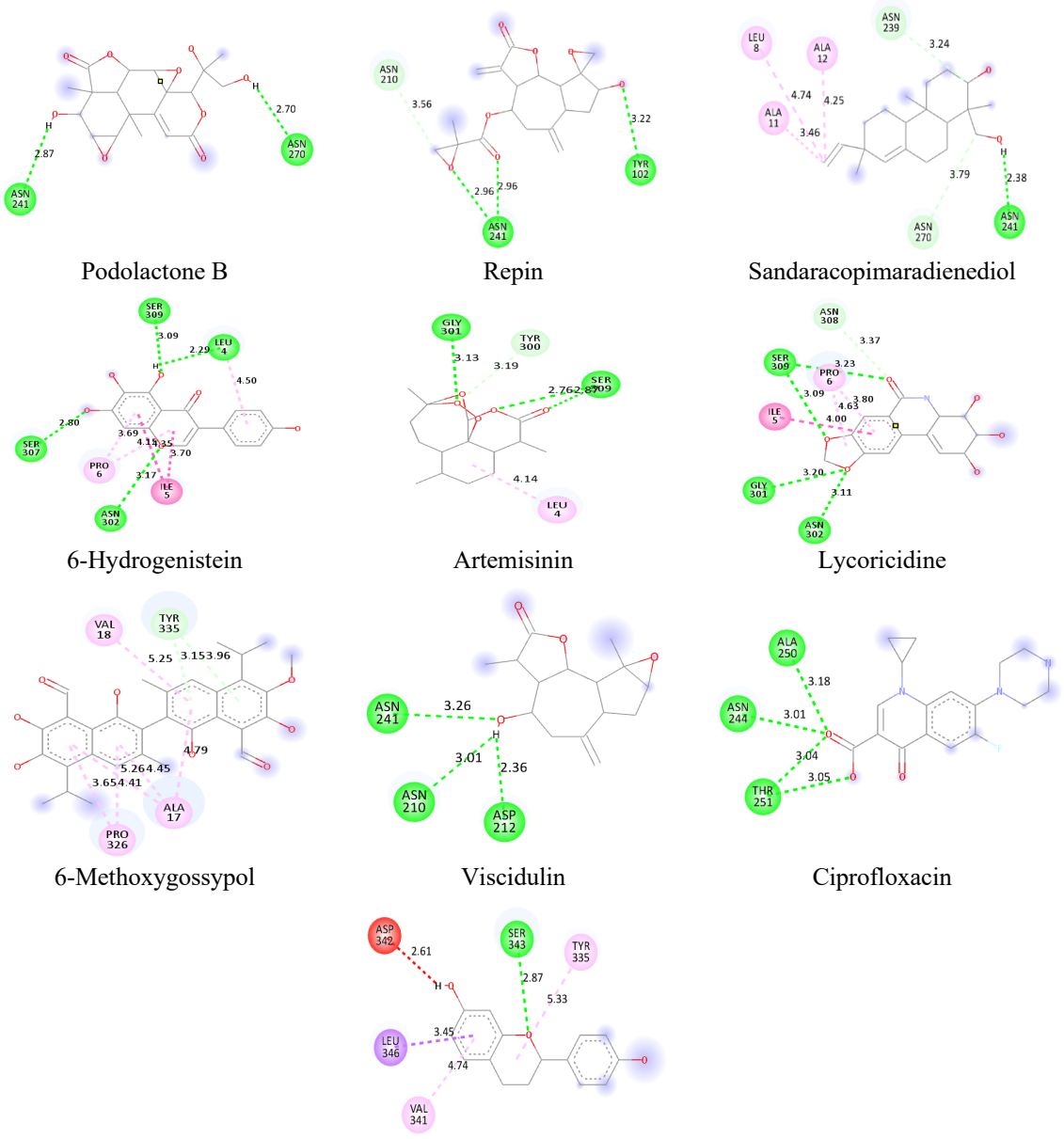

Figure 1. Interaction maps of the candidate biofungicides.

Conclusion

Pathogenic fungi cause various diseases in plants, reducing product productivity in many types of vegetables and fruits, or having the potential to completely destroy the product before or after harvest by causing powdery mildew, root rot or blight, and gray mold formation in the host organisms.

As a result of the studies and analysis of the findings, L-323 (Podolactone B), L-340 (Repin), L-353 (Sandaracopimaradienediol), L-28 (6-Hydrogenistein), L-71 (Artemisinin), L-259 (Lycoricidine), L-29 (6-Methoxygossypol), L-400 (Viscidulin), L-128 (Ciprofloxacin), L-31 (7,4'-Dihydroxyflavan) were determined as candidate biofungicide active molecules among 409 plant active molecules *in silico* characterization for PME inhibition of *B. cinerea* pest.

With the development of new strategies for the production of organic-based bio-pesticides in the biocontrol of plant pathogenic fungi, is expected to make significant contributions to the literature, especially with the increase in molecular-based studies of host adaptation and plant resistance aimed at maintaining plant resistance in a more sustainable manner. Initiating these researches within silico-based studies will contribute to experimental studies in terms of both time and cost.

Ethical Statement

Ethical approval is not required for this study.

Conflict of Interest

The Author(s) declare(s) that there are no conflicts of interest.

Funding Statement

The authors did not receive support from any organization for the submitted work.

References

Abbey, J. A., Percival, D., Abbey, L., Asiedu, S. K., Prithiviraj, B., & Schilder, A. (2019). Biofungicides as alternative to synthetic fungicide control of grey mould (Botrytis cinerea)–prospects and challenges. *Biocontrol science and technology*, *29*(3), 207-228.

Atalay, V. E., & Asar, S. (2024). Determination of the inhibition effect of hesperetin and its derivatives on Candida glabrata by molecular docking method. *The European Chemistry and Biotechnology Journal*, (1), 27-38

BIOVIA, D. S. (2021). Discovery Studio Visualizer; v21. 1.0. 20298 Dassault Systèmes: San Diego. *CA, USA*.

Bock, C. H., Barbedo, J. G., Del Ponte, E. M., Bohnenkamp, D., & Mahlein, A. K. (2020). From visual estimates to fully automated sensor-based measurements of plant disease severity: status and challenges for improving accuracy. *Phytopathology Research*, *2*, 1-30.

Boukaew, S., Prasertsan, P., Troulet, C., & Bardin, M. (2017). Biological control of tomato gray mold caused by Botrytis cinerea by using Streptomyces spp. *BioControl*, *62*, 793-803.

Chilvers, M. I., & du Toit, L. J. (2006). Detection and identification of Botrytis species associated with neck rot, scape blight, and umbel blight of onion. *Plant Health Progress*, *7*(1), 38.

Chun, S. W., Song, D. J., Lee, K. H., Kim, M. J., Kim, M. S., Kim, K. S., & Mo, C. (2024). Deep learning algorithm development for early detection of Botrytis cinerea infected strawberry fruit using hyperspectral fluorescence imaging. Postharvest Biology and Technology, 214, 112918.

Daina, A., Michielin, O., & Zoete, V. (2017). SwissADME: a free web tool to evaluate pharmacokinetics, drug-likeness and medicinal chemistry friendliness of small molecules. *Scientific reports*, *7*(1), 42717.

Dean, R., Van Kan, J. A., Pretorius, Z. A., Hammond-Kosack, K. E., Di Pietro, A., Spanu, P. D., ... & Foster, G. D. (2012). The Top 10 fungal pathogens in molecular plant pathology. *Molecular plant pathology*, *13*(4), 414-430.

Demirel, S., Usta, M., & Güller, A. (2022). In silico analysis of ribosome-inactivating protein (tritin) from common wheat plants (Triticum aestivum L.). Avrupa Bilim Ve Teknoloji Dergisi(33), 79-87.

Diab, M. K., Mead, H. M., Khedr, M. A., Nafie, M. S., Abu-Elsaoud, A. M., & El-Shatoury, S. A. (2024). Metabolite profiling and in-silico studies show multiple effects of insecticidal actinobacterium on Spodoptera littoralis. Scientific Reports, 14(1), 3057.

Duke, J. A. (2020). *Database of biologically active phytochemicals & their activity*. CRC Press.

Eberhardt, J., Santos-Martins, D., Tillack, A. F., & Forli, S. (2021). AutoDock Vina 1.2. 0: New docking methods, expanded force field, and python bindings. Journal of chemical information and modeling, 61(8), 3891-3898.

Elad, Y., Williamson, B., Tudzynski, P., & Delen, N. (Eds.). (2004). *Botrytis: biology, pathology and control*. Springer Science & Business Media.

Ez-Zoubi, A., Ez Zoubi, Y., Bentata, F., El-Mrabet, A., Ben Tahir, C., Labhilili, M., & Farah, A. (2023). Preparation and characterization of a biopesticide based on artemisia herba-alba essential oil encapsulated with succinic acid-modified beta-cyclodextrin. *Journal of Chemistry*, *2023*(1), 3830819.

Hawthorne, B. T. (1988). Fungi causing storage rots on fruit of Cucurbita spp. *New Zealand journal of experimental agriculture*, *16*(2), 151-157.

Hehre, W. J. (2003). *A guide to molecular mechanics and quantum chemical calculations* (Vol. 2). Irvine, CA: Wavefunction.

Jumper, J., Evans, R., Pritzel, A., Green, T., Figurnov, M., Ronneberger, O., ... & Hassabis, D. (2021). Highly accurate protein structure prediction with AlphaFold. *Nature*, *596*(7873), 583-589.

Karakaya, A., & Bayraktar, H. (2009). Botrytis disease of kiwifruit in Turkey. *Australasian Plant Disease Notes*, *4*(1), 87-88.

Kurbetli, İ., Aydoğdu, M., Sülü, G., & Polat, İ. (2016). First report of pre-harvest rot of pear fruit caused by Botrytis cinerea in Turkey. *New Disease Reports*, *34*(1), 16-16.

Latorre, B., Elfar Aedo, K., & Ferrada, E. E. (2015). Gray mold caused by Botrytis cinerea limits grape production in Chile. *Ciencia e Investigacion Agraria*, 42(3), 305-330.

Lipinski, C. A., Lombardo, F., Dominy, B. W., & Feeney, P. J. (1997). Experimental and computational approaches to estimate solubility and permeability in drug discovery and development settings. Advanced drug delivery reviews, 23(1-3), 3-25.

Mathew, D., Kumar, C. S., & Cherian, K. A. (2021). Foliar fungal disease classification in banana plants using elliptical local binary pattern on multiresolution dual tree complex wavelet transform domain. *Information processing in Agriculture*, *8*(4), 581-592.

Morris, G. M., Huey, R., Lindstrom, W., Sanner, M. F., Belew, R. K., Goodsell, D. S., & Olson, A. J. (2009). AutoDock4 and AutoDockTools4: Automated docking with selective receptor flexibility. *Journal of computational chemistry*, *30*(16), 2785-2791.

Nakajima, M., & Akutsu, K. (2014). Virulence factors of Botrytis cinerea. *Journal of General Plant Pathology*, *80*(1), 15-23.

Petrasch, S., Knapp, S. J., Van Kan, J. A., & Blanco-Ulate, B. (2019). Grey mould of strawberry, a devastating disease caused by the ubiquitous necrotrophic fungal pathogen Botrytis cinerea. *Molecular plant pathology*, *20*(6), 877-892.

Pimentel, D., Krummel, J., Gallahan, D., Hough, J., Merrill, A., Schreiner, I., ... & Fiance, S. (1978). Benefits and costs of pesticide use in US food production. *BioScience*, *28*(12), 772-784.

Pimentel, D., McLaughlin, L., Zepp, A., Lakitan, B., Kraus, T., Kleinman, P., ... & Selig, G. (1991). Environmental and economic effects of reducing pesticide use. *BioScience*, *41*(6), 402-409.

Prusky, D., & Lichter, A. (2007). Activation of quiescent infections by postharvest pathogens during transition from the biotrophic to the necrotrophic stage. *FEMS microbiology letters*, *268*(1), 1-8.

Rojas, D. S., & Gilbert, G. S. (2024). The response of botrytis cinerea to fire in a coast redwood forest. *International Journal of Plant Biology*, *15*(1), 94-101.

Sadek, M. E., Shabana, Y. M., Sayed-Ahmed, K., & Abou Tabl, A. H. (2022). Antifungal activities of sulfur and copper nanoparticles against cucumber postharvest diseases caused by Botrytis cinerea and Sclerotinia sclerotiorum. *Journal of Fungi*, *8*(4), 412.

Stahl, M., & Rarey, M. (2001). Detailed analysis of scoring functions for virtual screening. *Journal of medicinal chemistry*, *44*(7), 1035-1042.

Stahr, M. N., & Quesada-Ocampo, L. M. (2019). Black rot of sweetpotato: A comprehensive diagnostic guide. *Plant health progress*, *20*(4), 255-260.

Sun, K., van Tuinen, A., van Kan, J. A., Wolters, A. M. A., Jacobsen, E., Visser, R. G., & Bai, Y. (2017). Silencing of DND1 in potato and tomato impedes conidial germination, attachment and hyphal growth of Botrytis cinerea. *BMC plant biology*, *17*, 1-12.

Sunil, C. K., Jaidhar, C. D., & Patil, N. (2023). Systematic study on deep learning-based plant disease detection or classification. Artificial Intelligence Review, 56(12), 14955-15052.

TOB. (2023). *Tarım ve Orman Bakanlığı Bitki Koruma Ürünleri Daire Başkanlığı*. Retrieved 10.10.2023 from https://bku.tarimorman.gov.tr/Zararli/Details/1252

Usta, Mustafa & Güller, Abdullah & Demirel, Serap & Korkmaz, Gülüstan & Kurt, Zeynelabidin. (2023). New insights into tomato spotted wilt orthotospovirus (TSWV) infections in Türkiye: Molecular detection, phylogenetic analysis, and in silico docking study. *Notulae Botanicae Horti Agrobotanici Cluj-Napoca*, *51*(3), 13245-13245.

Valette-Collet, O., Cimerman, A., Reignault, P., Levis, C., & Boccara, M. (2003). Disruption of Botrytis cinerea pectin methylesterase gene Bcpme1 reduces virulence on several host plants. *Molecular Plant-Microbe Interactions*, *16*(4), 360-367.

Viret, O., Keller, M., Jaudzems, V. G., & Cole, F. M. (2004). Botrytis cinerea infection of grape flowers: light and electron microscopical studies of infection sites. *Phytopathology*, *94*(8), 850-857.

Vivekanandhan, P., Alharbi, S. A., & Ansari, M. J. (2024). Toxicity, biochemical and molecular docking studies of Acacia nilotica L., essential oils against insect pests. *Toxicon*, *243*, 107737.

Wang, L., Hu, J., Li, D., Reymick, O. O., Tan, X., & Tao, N. (2022). Isolation and control of Botrytis cinerea in postharvest green pepper fruit. *Scientia Horticulturae*, *302*, 111159.

Williamson, B., Tudzynski, B., Tudzynski, P., & Van Kan, J. A. (2007). Botrytis cinerea: the cause of grey mould disease. *Molecular plant pathology*, *8*(5), 561-580.

Wyss, P. C., Gerber, P., Hartman, P. G., Hubschwerlen, C., Locher, H., Marty, H. P., & Stahl, M. (2003). Novel dihydrofolate reductase inhibitors. Structure-based versus diversity-based library design and high-throughput synthesis and screening. *Journal of medicinal chemistry*, *46*(12), 2304-2312.

Xiao, C. L. (2006). Postharvest fruit rots in d'Anjou pears caused by Botrytis cinerea, Potebniamyces pyri, and Sphaeropsis pyriputrescens. *Plant health progress*, *7*(1), 40.

Youssef, K., de Oliveira, A. G., Tischer, C. A., Hussain, I., & Roberto, S. R. (2019). Synergistic effect of a novel chitosan/silica nanocomposites-based formulation against gray mold of table grapes and its possible mode of action. *International journal of biological macromolecules*, *141*, 247-258.